Histol Histopathol (2018) 33: 89-99

http://www.hh.um.es

Histology and Histopathology

From Cell Biology to Tissue Engineering

Zoledronate promotes bone formation by blocking osteocyte-osteoblast communication during bone defect healing

Pingping Cui[1], Hongrui Liu[1], Jing Sun[1], Norio Amizuka[2], Qinfeng Sun[1] and Minqi Li[1]

[1]Department of Bone Metabolism, School of Stomatology Shandong University, Shandong Provincial Key Laboratory of Oral Tissue Regeneration, Jinan, China and [2]Department of Developmental Biology of Hard Tissue, Graduate School of Dental Medicine, Hokkaido University, Sapporo, Japan

Summary. Nitrogen-containing bisphosphonates (N-BPs) are potent antiresorptive drugs and their actions on osteoclasts have been studied extensively. Recent studies have suggested that N-BPs also target bone-forming cells. However, the precise mechanism of N-BPs in osteoblasts is paradoxical, and the specific role of osteocytes is worthy of in-depth study. Here, we investigated the cellular mechanisms of N-BPs regulating bone defect healing by zoledronate (ZA). Bone histomorphometry confirmed an increase in new bone formation by systemic ZA administration. ZA induced more alkaline phosphatase-positive osteoblasts and tartrate-resistant acid phosphatase-positive osteoclasts residing on the bone surface. Inexplicably, ZA increased SOST expression in osteocytes embedded in the bone matrix, which was not compatible with the intense osteoblast activity on the bone surface. ZA induced heterogeneous osteocytes and disturbed the distribution of the osteocytic-canalicular system (OLCS). Furthermore, according to the degree of OLCS regularity, dentin matrix protein 1 reactivity had accumulated around osteocytes in the ZA group, but it was distributed evenly in the OLCS of the control group. The control group showed a dense array of the gap junction protein connexin 43. However, connexin 43 was extremely sparse after ZA administration. In summary, ZA treatment reduces gap junction connections and blocks cellular communication between osteocytes and osteoblasts. Retaining SOST expression in osteocytes leads to activation of the Wnt signaling pathway and subsequent bone formation.

Key words: Zoledronate, Osteoblasts, Osteocytes, Connexin 43, Bone defect

Offprint requests to: Qinfeng Sun, DDS, PhD, School of Stomatology Shandong University, Shandong Provincial Key Laboratory of Oral Tissue Regeneration, Wenhua West Road 44-1, Jinan 250012, China. e-mail: sunqinfeng@sdu.edu.cn or Minqi Li, DDS, PhD, Department of Bone Metabolism, School of Stomatology Shandong University, Shandong Provincial Key Laboratory of Oral Tissue Regeneration, Wenhua West Road 44-1, Jinan 250012, China. e-mail: liminqi@sdu.edu.cn

DOI: 10.14670/HH-11-893

Introduction

Because of its potent antiresorptive effects, zoledronate (ZA) is a commonly used nitrogen-containing bisphosphonate (N-BP) for bone metastasis treatment (Chen and Fu, 2002). It shares most commonalities of N-BPs, such as inhibiting the critical enzyme farnesyl pyrophosphate synthase in the mevalonate pathway (Rogers, 2003) and suppressing prenylation of small GTPases (Luckman et al., 1998), which are essential for cytoskeletal organization of osteoclasts, finally affecting osteoclast survival (Palokangas et al., 1997; Abu-Amer et al., 1999). Indeed, it has been demonstrated that N-BPs prevent differentiation of macrophages into osteoclasts, block the activity of mature osteoclasts, induce osteoclast apoptosis (Rodan, 1998; Rogers et al., 2000), and reduce the number of osteoclasts (Tanaka et al., 2010). Thus far, bone-resorbing osteoclasts have long been thought to be the primary target of N-BPs.

N-BPs may also target other cell types such as bone-forming osteoblasts. They have been reported to

stimulate osteoblast proliferation, early osteoblastogenesis, and osteoblast differentiation *in vitro* (Giuliani et al., 1998; Lindtner et al., 2014). Local application of N-BPs promotes bone formation and improves bone structures *in vivo* (Tanzer et al., 2005; Gao et al., 2009; Günes et al., 2016). Previously, our group demonstrated that systemic administration of N-BPs increases osteoblastic activity and the trabecular volume of tibiae in mice (Liu et al., 2015). Consistently, ZA treatment promotes new bone formation in osteoporotic rats (Mardas et al., 2017). In addition, ZA enhances new bone formation by autogenous bone grafting in the rat calvarial defect model (Toker et al., 2012). In terms of the precise biological mechanisms of this anabolic action in bone, the antiapoptotic effects of N-BPs on osteoblasts through extracellular signal-regulated kinase signaling provides a rational explanation (Bellido and Plotkin, 2011). However, during physiological bone remodeling, bone formation continuously occurs on bone surfaces along with resorption pits, a process referred as "osteoclast-osteoblast coupling" (Crane et al., 2016). Therefore, the inhibition of osteoclastic bone resorption induced by N-BPs should cause a reduction in both osteoblastic activity and bone formation (Tsuboi et al., 2016). Such an assumption supports previous reports showing that N-BPs inhibit bone nodule formation and bone mineralization in rats (Iwata et al., 2006; Corrado et al., 2010). Taken together, the paradoxical roles of N-BPs in osteoblastic activity and the precise mechanism of N-BPs in bone remodeling are worthy of in-depth study.

Moreover, there is the possibility that indirect effects from osteocytes embedded within the bone matrix may be involved in the regulation of bone remodeling by N-BPs. Osteocytes, which account for 90% of bone cells, lie among osteocytic lacunae and stretch out thin cytoplasmic processes that pass through narrow osteocytic canaliculi, forming the osteocyte lacunar canalicular system (OLCS) (Hirose et al., 2007). The OLCS not only senses mechanical/hormonal stimuli, but also coordinates the functions of osteoblasts and osteoclasts (Hirose et al., 2007). Our previous study suggested that osteocyte ablation causes corresponding changes in osteoblasts, osteoclasts, and bone matrix mineralization by analyzing the diphtheria toxin receptor transgenic mouse model (Tatsumi et al., 2007; Li et al., 2013). Importantly, osteoblasts and osteocytes connect their cytoplasmic processes via gap junctions (Stains and Civitelli, 2005; Stains et al., 2014), thereby forming a functional syncytium. From another aspect, N-BPs prevent osteocyte apoptosis (Follet et al., 2007), modify the osteocyte channel arrangement (Rabelo et al., 2015), and regulate expression of osteocyte-specific factors such as dentin matrix protein 1 (DMP-1) and PHEX (Yao et al., 2008). Thus, it is plausible that N-BPs may at least partly regulate the biological activities of osteoblasts through osteocytes.

Optimal repair of skeletal tissue is necessary in all varieties of elective and reparative orthopedic surgical treatments (Gerstenfeld et al., 2003). However, postnatal skeletal repair is unique because it requires bone modeling in which preosteoblasts are recruited to form bone, followed by prolonged bone remodeling involving osteoclastic bone resorption and coupled bone formation (Phillips, 2005). Bone trauma destroys the normal microenvironment and is usually considered to be a major risk factor for clinical use of N-BPs (Yu et al., 2012). The interaction between different cell populations and their microenvironment forms the specific nature of the site of bone trauma (Gerstenfeld et al., 2003). Under these circumstances, we performed bone defect surgery combined with systemic ZA administration to explore the effects of N-BPs on bone defect healing, and the behavior of osteoclasts, osteoblasts, and osteocytes in mice at 8 weeks after continuation of weekly ZA administration.

Materials and methods

Animal model establishment and tissue preparation

All animal experiments in this study were conducted according to the Guidelines for Animal Experimentation of the School of Stomatology, Shandong University. Twenty 8-week old male mice (KM strain) were obtained from Animal Centre of Shandong University (Jinan, China) and kept in plastic cages (3-5 animals per cage) under standard laboratory conditions with a 12h dark, 12h light cycle and a constant temperature of 20°C and humidity of 48%. All mice were fed a standard rodent diet ad libitum. Under general anesthesia with an intraperitoneal injection of 10% chloral hydrate (400 mg/l00g body weight), skin incisions were made along the right femurs on lateral sides of the thighs of all animals, vastus lateralis muscle and rectus femoris muscle were carefully separated to expose the femur. A 3mm×5mm×lmm (width×length×depth) bone defect was made by stainless fissure bur at the middle part of the anterior surface of the femur. Skin incisions were sutured carefully. All mice were randomly divided into two groups, ZA-administered group and control group (n=l0). To prepare ZA for administration, one vial of ZA (4 mg) (The pharmaceutical Co., Ltd, Anhui, China) was dissolved in 200 ml of physiological saline. According to one of our previous studies, we chose the amount of ZA to reproduce in mice the posology used for the therapy of bone metastases in humans (Liu et al., 2015). In ZA group, animals were administrated a weekly intravenous injection of ZA (125 μg/kg body weight) for up to 8 weeks. Control mice received physiological saline.

After 8 weeks, the animals were anesthetized with an intraperitoneal injection of 10% chloral hydrate (400 mg/l00g body weight) and fixed with 4% paraformaldehyde in 0.1 M phosphate buffer (pH 7.4) by transcardial perfusion. After fixation, femurs were removed and immersed in the same fixative for an additional 24 h. Following that, samples were

decalcified with 10% EDTA-2Na solution for 3 weeks at 4°C. Then the specimens were dehydrated through an ascending ethanol series and then embedded in paraffin using standard procedures. Serial longitudinal 5-μm-thick sections were prepared for following histological analysis using sliding microtome (LEICA SM 2010R, Heidelberger, German).

Histological examination and image analysis

Hematoxylin and eosin (H&E) staining was performed to investigate the morphology of bone defect area in both groups. Stained sections were observed and digital images were taken with a light microscope (Olympus BX-53, Tokyo, Japan). The newly formed bone volume, expressed as a percentage (area of newly formed bone/area of original wound (defect) ×100%), was measured at an original magnification of ×40 by Image Pro Plus 6.2 software (Media Cybernetics, Silver Spring, MD). Specifically, bone defect area was defined from histologically visible cut edge of cortical bone and newly formed bone was identified by its woven structure. Ultimately, 10 slices of each sample were used for quantitative histomorphometric analysis to get the mean value.

Immunohistochemical (ALP, SOST, DMPJ, and Connexin 43) and Histochemistry (TRAP) examination

For immunolocalization of ALP, SOST, DMPl and Connexin 43, serial 5 μm-thick paraffin sections were dewaxed in xylene and rehydrated in ethanol series. Endogenous peroxidases were blocked by incubation sections in 0.3% hydrogen peroxide for 30 min at room temperature. Then sections were preincubated with 1% bovine serum albumin in phosphate-buffered saline (BSA-PBS) for 20 min to reduce non-specific staining. The sections were then incubated for 2 h at room temperature with: 1) rabbit antiserum nonspecific ALPase, generated by Oda et al. (1999) at a dilution of 1:100; 2) anti-SOST antibody (R&D Systems, Minneapolis, MN, USA) at a dilution of 1:50; 3) anti-DMP-1 antibody (Millipore, Boston, MA, USA) at a dilution of 1:50; and 4) anti-Connexin 43 antibody (Proteintech Group, inc, Chicago, MI, USA) at a dilution of 1:50 in 1% BSA-PBS. After rinsing with PBS, sections were incubated with horseradish peroxidase-conjugated swine anti-rabbit IgG (Dako, Glostrup, Denmark) for ALP and Connexin-43; rabbit anti-goat IgG (Jackson ImmunoResearch Laboratories, Baltimore, MD, USA) for SOST; and goat anti-mouse IgG (Jackson ImmunoResearch Laboratories, Baltimore, MD, USA) for DMP-1 at a dilution of 1:100 for 1 h at room temperature. The immunoreaction was visualized with diaminobenzidine (DAB) (Sigma-Aldrich, St. Louis, MO, USA). All sections were counterstained faintly with methyl green and observed under a light microscope (Olympus BX-53; Olympus, Tokyo, Japan).

Tartrate-resistant acid phosphatase (TRAP) staining was performed as previously shown (Li et al., 2013). In brief, sections were submerged in a mixture of 3.0 mg of naphthol AS-BI phosphate, 18 mg of red violet LB salt, and 100 mM L(+) tartaric acid (0.36 g) diluted in 30 ml of 0.1 M sodium acetate buffer (pH 5.0) for 15 min at 37°C. The sections were then faintly counterstained with methyl green for assessing by light microscopy (Olympus BX-53, Tokyo, Japan).

For double immunostaining with SOST/ALP and DMPl/ALP, we at first performed SOST or DMP-1 immunohistochemistry visualizing using DAB, and then, ALP detection by employing enzyme histochemistry. In brief, the sections with the immune complex were incubated in an aquenous mixture of 2.5 mg of naphthol AS-BI phosphate(Sigma) and 18mg of fast blue RR salt (Sigma) diluted in 30ml of 0.1M Tris-HCL buffer (pH 8.5) for 30 min at 37°C. Double stained sections carrying SOST/DMPl (brown) and ALP (blue) were finally counterstained faintly with methyl green.

Statistically, ten tissue sections were selected from each sample. SOST-positive osteocytes numbers were counted; the mean optical density of ALP was measured in three randomly selected non-overlapping microscopic fields from each section by Image-Pro Plus 6.2 software.

Statistical analysis

All statistical analyses were performed using SPSS software. Values are presented as the mean ± standard deviation. Differences among groups were assessed by the unpaired t test. $P<0.05$ was considered statistically significant.

Results

Histological alterations during bone defect restoration

At 8 weeks' post-surgery, the new bone featured thicker trabeculae and almost covered the entire bone defect area. A meshwork of new bone with large bone marrow cavities was found in the control group (Fig. 1A). ZA treatment induced an increase in newly formed bone, which was accompanied by prominent remnants of uncalcified cartilage (Fig. 1B). In the ZA group, the newly formed bone often connected into a sheet, and bone marrow cavities were much smaller. As shown in Fig. 1C, statistical analysis revealed significant differences between ZA and control groups in terms of the newly formed bone volume (59.3±2.17 in the control group vs 86.2±1.97 in the ZA group, $P<0.001$).

Effects of ZA treatment on osteoblasts and osteoclasts

As shown in Fig. 2, alkaline phosphatase (ALP) was faintly expressed in the control group, but obviously detected on the surface of newly formed bone in the ZA group (Fig. 2A,B). Several small osteoclasts with

uniform morphology were found on the bone surface in the control group (Fig. 2A), whereas numerous large osteoclasts exhibited varying degrees of polymorphism in ZA-administered mice (Fig. 2B). Statistically, ALP activity (0.130±0.018 in the control group vs 0.262±0.019 in the ZA group, P<0.001) was increased after ZA treatment (Fig. 2C). These results suggested that ZA promoted bone regeneration.

ZA induces higher SOST expression with irreconcilable ALP activity

Osteocytes of the control group were uniform and arranged regularly with faint expression of SOST (Fig. 3A). However, osteocytes of the ZA group were heterogeneous and arranged disorderly with strong immunostaining of SOST (Fig. 3B). Moreover,

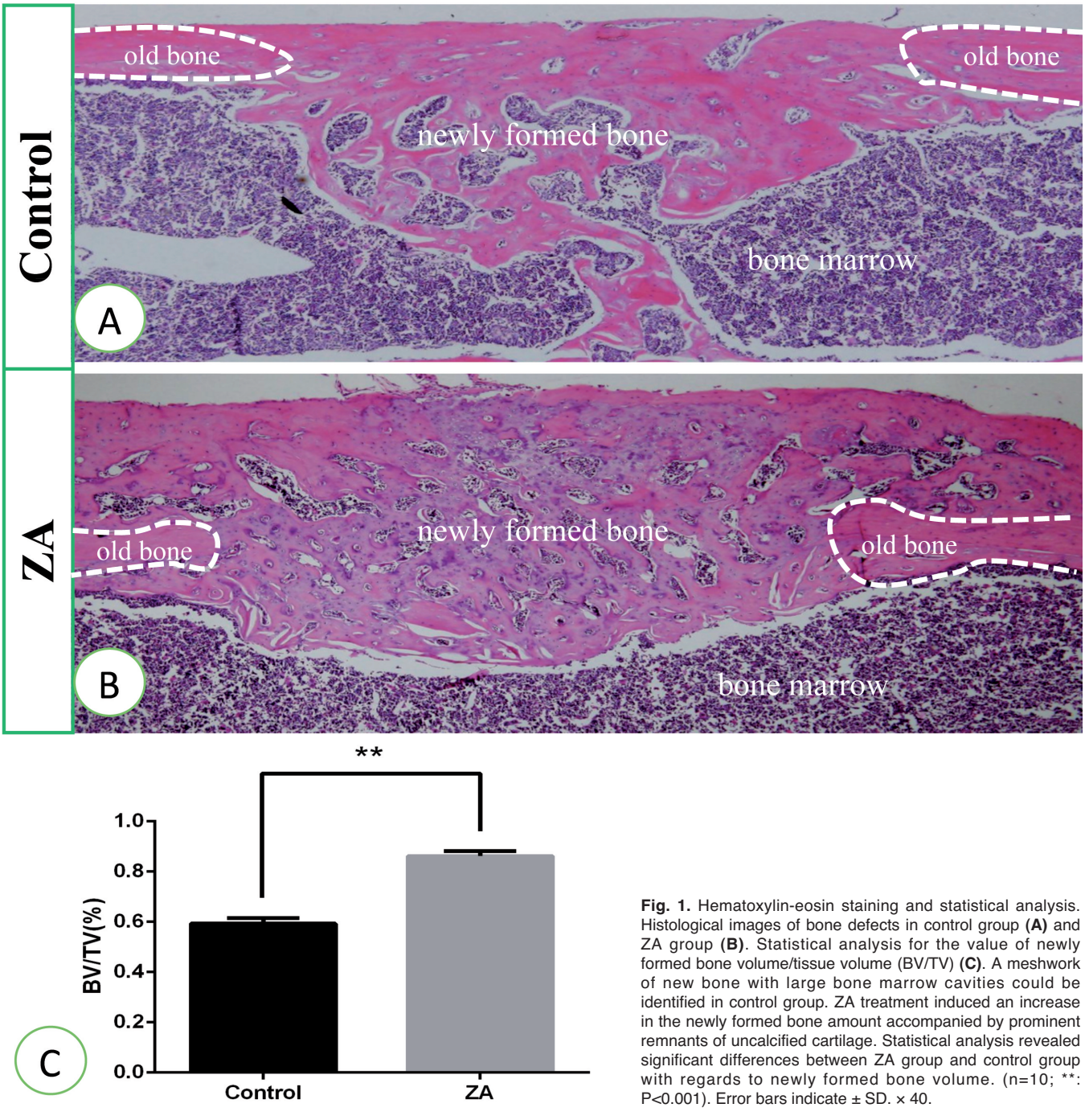

Fig. 1. Hematoxylin-eosin staining and statistical analysis. Histological images of bone defects in control group **(A)** and ZA group **(B)**. Statistical analysis for the value of newly formed bone volume/tissue volume (BV/TV) **(C)**. A meshwork of new bone with large bone marrow cavities could be identified in control group. ZA treatment induced an increase in the newly formed bone amount accompanied by prominent remnants of uncalcified cartilage. Statistical analysis revealed significant differences between ZA group and control group with regards to newly formed bone volume. (n=10; **: P<0.001). Error bars indicate ± SD. × 40.

expression of ALP was enhanced on the surface of newly formed bone. Statistical analysis showed obviously higher SOST-positive osteocyte numbers/field in the ZA group than the control group (19.0±2.37 in the control group vs 64.8±3.76 in the ZA group, P<0.001) (Fig. 3C). It is very perplexing that, although osteocytes expressed abundant SOST, ZA could still stimulate osteoblast activity and promote new bone formation.

Effects of ZA treatment on the osteocytic canalicular system

DMP-1 is an osteocyte-secreted factor that is also found in the osteocytic canalicular system. Histochemically, we assessed osteocyte morphology and the OLCS distribution by DMP-1/ALP double immunostaining. As shown in Fig. 4, in the control group, osteocytes showed a uniform morphology with an abundant OLCS arranged regularly (Fig. 4A,C). ZA induced heterogeneous osteocytes and disturbed the distribution of the OLCS (Fig. 4B,D). The OLCS in the control group extended from osteocytes to the bone surface (Fig. 4A,C). However, in the ZA group, osteocytes mainly formed short and small protrusions that could not contact with the bone surface (Fig. 4B,D). Furthermore, according to the degree of OLCS regularity, DMP-1 reactivity had accumulated around osteocytes in the ZA group, but it was distributed evenly in the OLCS of the control group (Fig. 4A-D).

Effects of ZA treatment on connexin 43

Connexin 43 is a component of gap junctions that play important roles in cellular communication. In the control group, there was intense expression of connexin 43 arranged as a cluster in the newly formed bone (Fig. 5A,C). However, ZA treatment induced abnormal osteocytes with enlarged lacuna and a folded shape (Fig. 5B,D). Connexin 43 expression became sparse upon ZA treatment, which was consistent with the blocked communication between osteocytes and osteoblasts (Fig. 5B,D).

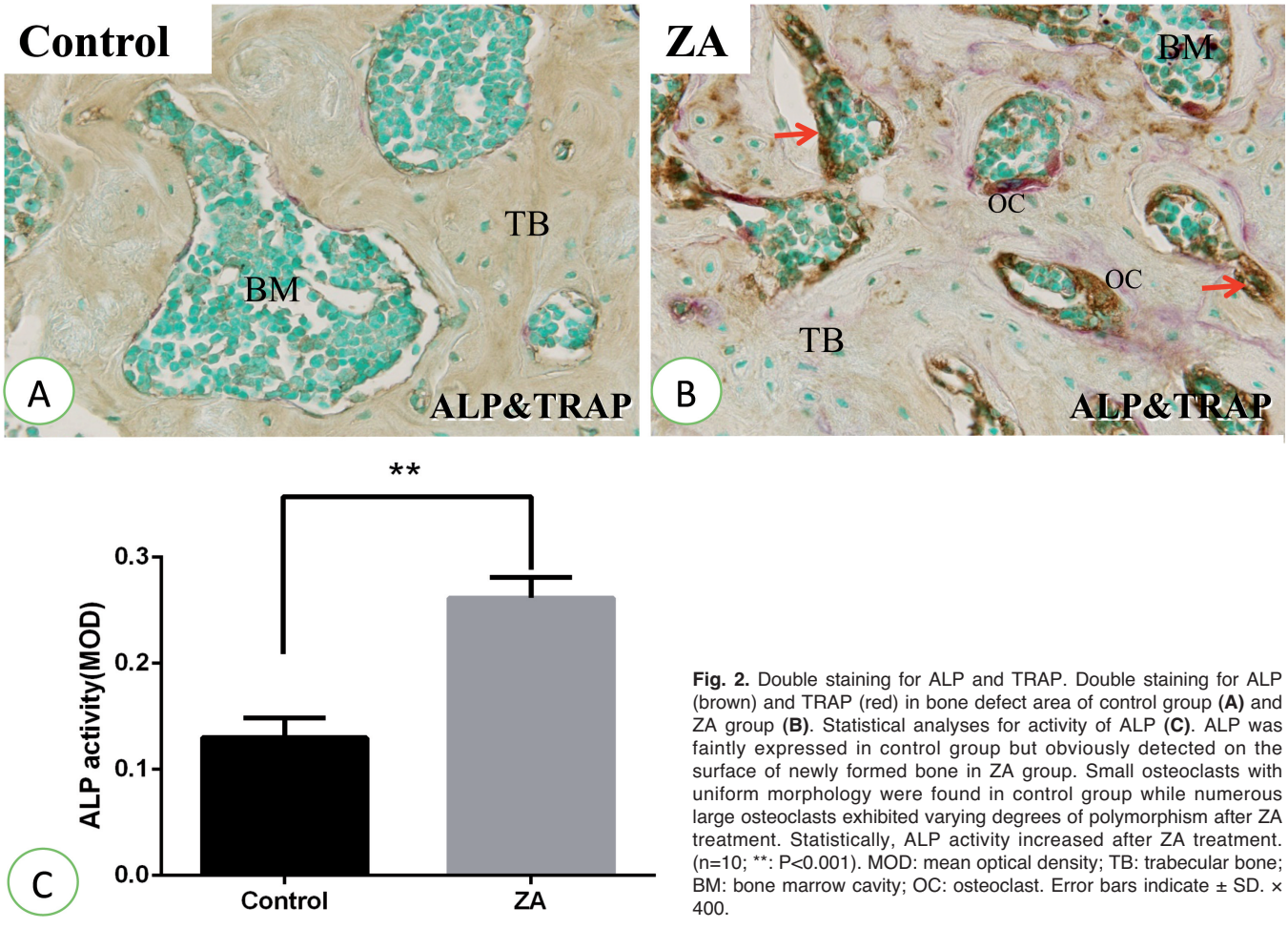

Fig. 2. Double staining for ALP and TRAP. Double staining for ALP (brown) and TRAP (red) in bone defect area of control group **(A)** and ZA group **(B)**. Statistical analyses for activity of ALP **(C)**. ALP was faintly expressed in control group but obviously detected on the surface of newly formed bone in ZA group. Small osteoclasts with uniform morphology were found in control group while numerous large osteoclasts exhibited varying degrees of polymorphism after ZA treatment. Statistically, ALP activity increased after ZA treatment. (n=10; **: P<0.001). MOD: mean optical density; TB: trabecular bone; BM: bone marrow cavity; OC: osteoclast. Error bars indicate ± SD. × 400.

Discussion

Systemic ZA administration induced more newly formed bone in the bone defect model of mice. By detecting alterations in osteoblasts and osteoclasts, we found that ZA induced an increase in the osteoclast number, which appears to be in contrast to the antiresorptive effect of N-BPs, and promoted bone regeneration. However, our previous report using the same dose of ZA showed induction of morphological changes in osteoclasts, a defective ruffled border, and a decrease in their adhesive ability (Liu et al., 2015). Thus, ZA may cause a decrease in the bone remodeling rate, which provides good evidence to explain the increase in immature bone structures of newly formed bone.

As a more important event during bone defect healing, bone formation is the central aim of this study. ZA enhanced ALP activity on the surface of newly formed bone. N-BPs either stimulate osteoblast precursor differentiation or inhibit *in vitro* osteoblast proliferation, depending on the type of N-BP, the concentration, and experimental model (Reinholz et al., 2000; Itoh et al., 2003). The coordinate increase in the number of osteoblasts and osteoclasts supported the hypothesis that osteoclastic bone resorption triggers the differentiation and activation of osteoblasts, a process referred to as a "coupling phenomenon" (Tsuboi et al., 2016) during bone remodeling. Alternatively, there is the possibility that ALP-immunopositive osteoblasts play a supporting role in osteoclast formation by simultaneously expressing RANKL (receptor activator of NF-κB ligand) (Liu et al., 2015). This result may partly explain the increase in osteoclast numbers and asymmetric resorption activity.

An increasing number of studies are suggesting that osteocytes are the regulation center of bone remodeling (Rochefort et al., 2010). Secretion of a variety of factors by osteocytes coordinates osteoblast activity indirectly.

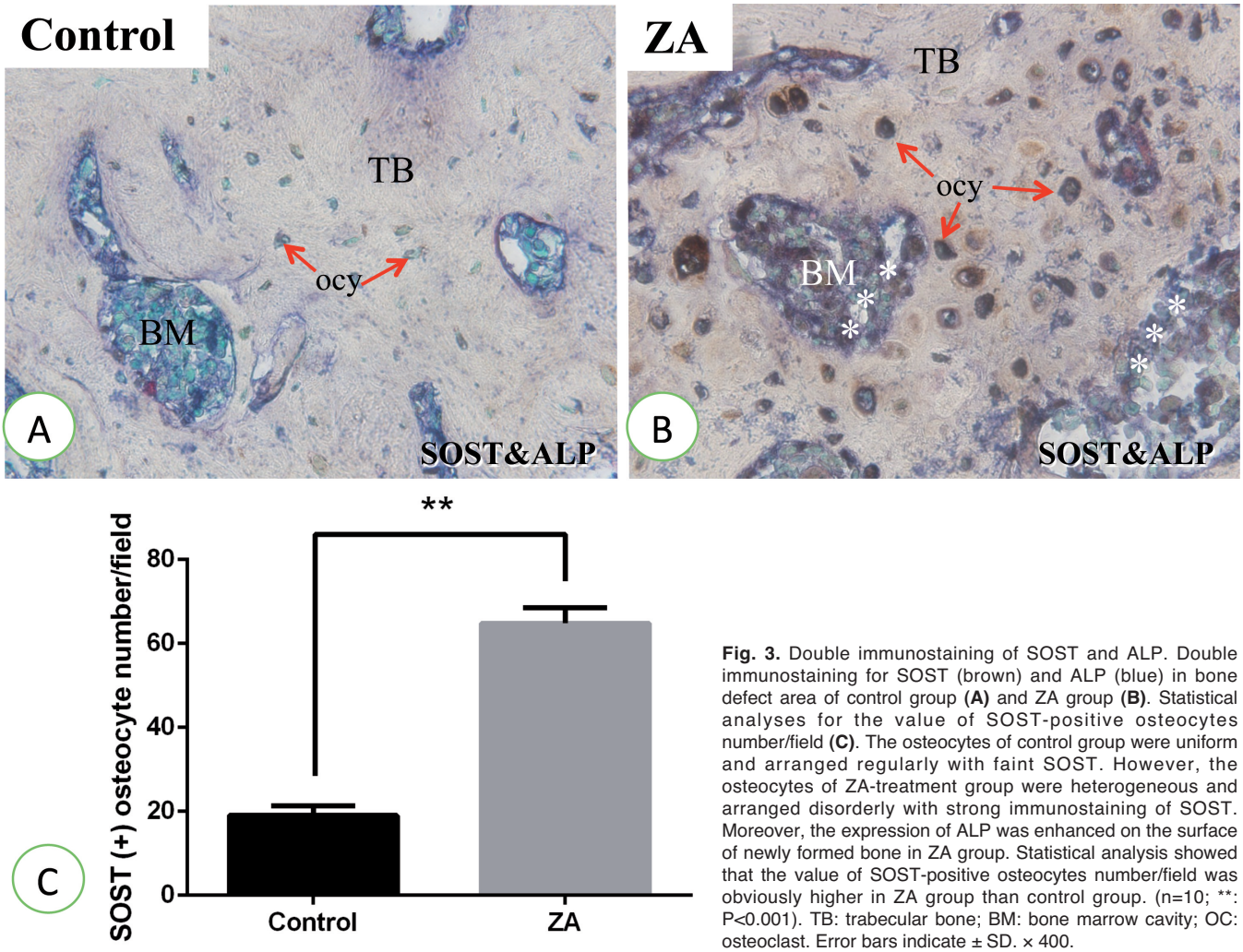

Fig. 3. Double immunostaining of SOST and ALP. Double immunostaining for SOST (brown) and ALP (blue) in bone defect area of control group **(A)** and ZA group **(B)**. Statistical analyses for the value of SOST-positive osteocytes number/field **(C)**. The osteocytes of control group were uniform and arranged regularly with faint SOST. However, the osteocytes of ZA-treatment group were heterogeneous and arranged disorderly with strong immunostaining of SOST. Moreover, the expression of ALP was enhanced on the surface of newly formed bone in ZA group. Statistical analysis showed that the value of SOST-positive osteocytes number/field was obviously higher in ZA group than control group. (n=10; **: P<0.001). TB: trabecular bone; BM: bone marrow cavity; OC: osteoclast. Error bars indicate ± SD. × 400.

SOST inhibits bone formation by antagonizing several members of the bone morphogenetic protein family and binds to LRP5/LRP6, thereby inhibiting canonical Wnt signaling (Winkler et al., 2003). Loss of SOST expression in humans leads to bone disorders, such as sclerosteosis, which are characterized by progressive skeletal overgrowth (Balemans et al., 2001). Targeted deletion of the SOST gene in mice leads to increased bone formation and bone strength (Li et al., 2008). Although it is clear that osteocytes inhibit osteogenesis through the secretion of SOST, our results showed that a reduction of SOST expression in osteocytes caused an increase in osteoblast activity on the new bone surface, which is perplexing.

Osteocytes establish the functional osteocytic canalicular system that plays crucial roles during matter exchange and mechanical stress sensing (Aarden et al., 1994; Burger and Klein-Nulend, 1999). The OLCS also regulates bone remodeling and mineral metabolism by affecting communication among osteocytes and between osteocytes and osteoblasts (Weinbaum et al., 1994; Feng et al., 2006; Tatsumi et al., 2007). Under physiological conditions, the OLCS usually exhibits a finely tuned arrangement, but it can be altered by physical or chemical imbalances (Masuki et al., 2010). Osteocyte-derived molecules may not only provide clues to understand osteocytic functions, but also reflect the biological roles of the OLCS. DMP-1, which is a bone matrix protein expressed in osteocytes, is widely accepted to regulate bone mineral homeostasis because of its high calcium ion-binding capacity (Toyosawa et al., 2001). Because DMP-1 has been identified in the

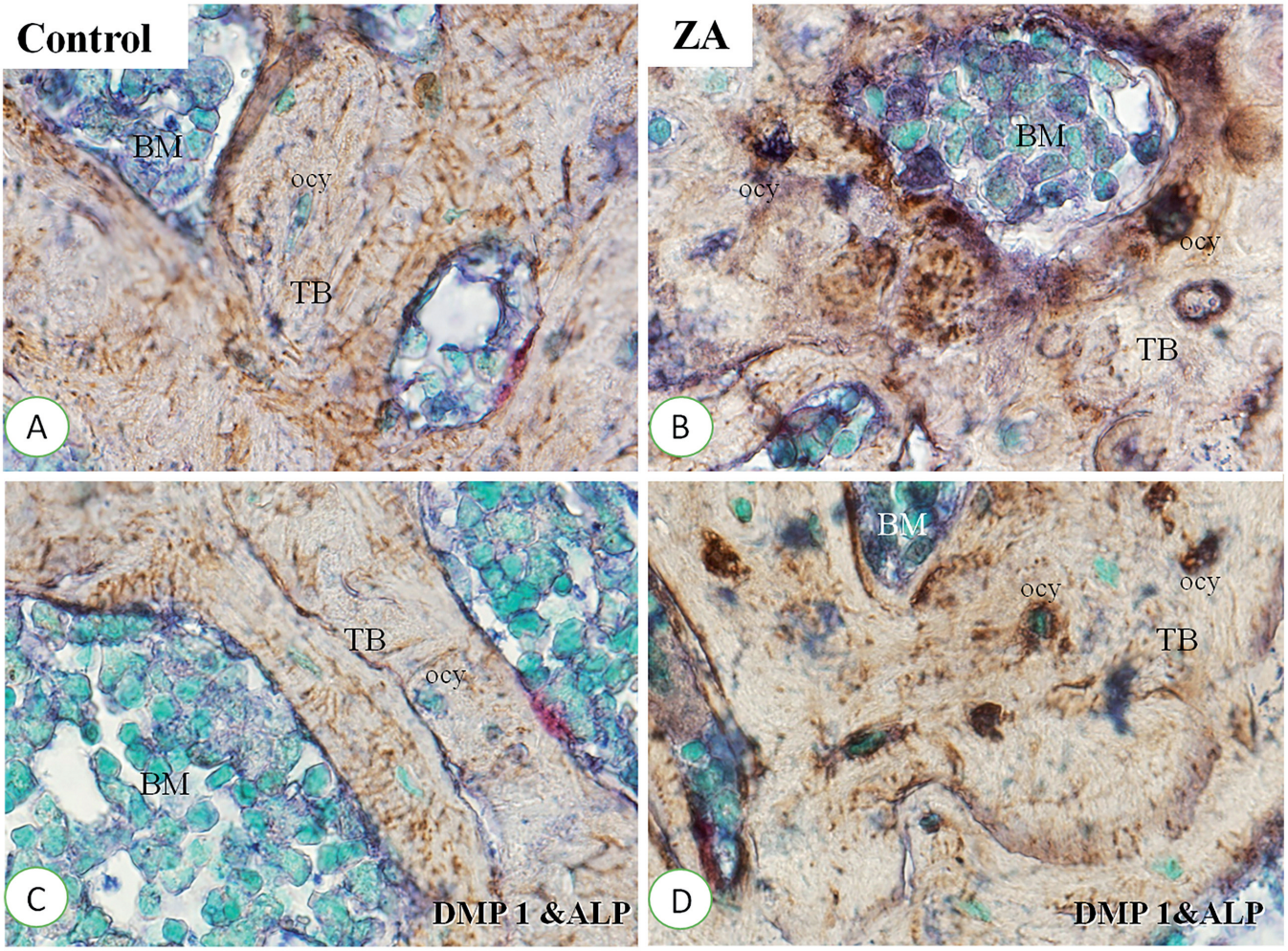

Fig. 4. Double immunostaining of DMP-1 and ALP. Double immunostaining for DMP1 (brown) and ALP (blue) in bone defect area of control group **(A, C)** and ZA group **(B, D)**. In control group, osteocytes showed uniform morphology with abundant OLCS which arranged regularly. ZA induced heterogeneous osteocytes and disturbed distribution of OLCS. DMP-1 reactivity was accumulated surrounding osteocytes in ZA group but it distributed evenly in OLCS in control group. TB: trabecular bone; BM: bone marrow cavity; Ocy: osteocyte. × 1000.

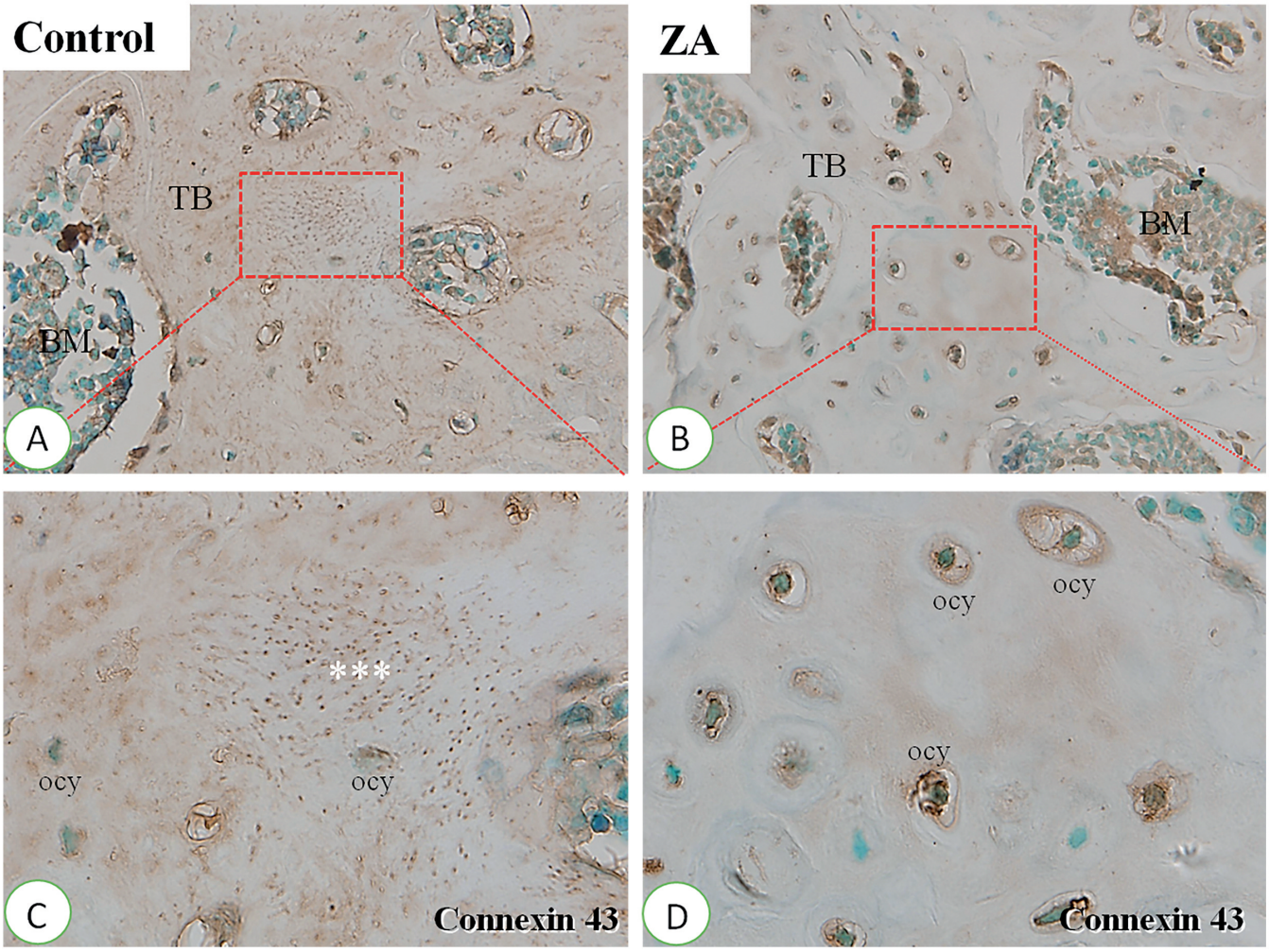

Fig. 5. Immunostaining of Connexin 43. Immunostaining of Connexin 43 in control group **(A)** and ZA group **(B).** The visual fields framed by the red line are magnified in the adjacent below images **(C, D)**. In the control group, there is intensive expression of Connexin 43 arranged in clusters in the newly formed bone. But, ZA treatment induced abnormal osteocytes with enlarged lacuna and folded shape with sparse Connexin 43 expression. TB: trabecular bone; BM: bone marrow cavity; Ocy: osteocyte. A, B, × 200; C, D, × 400.

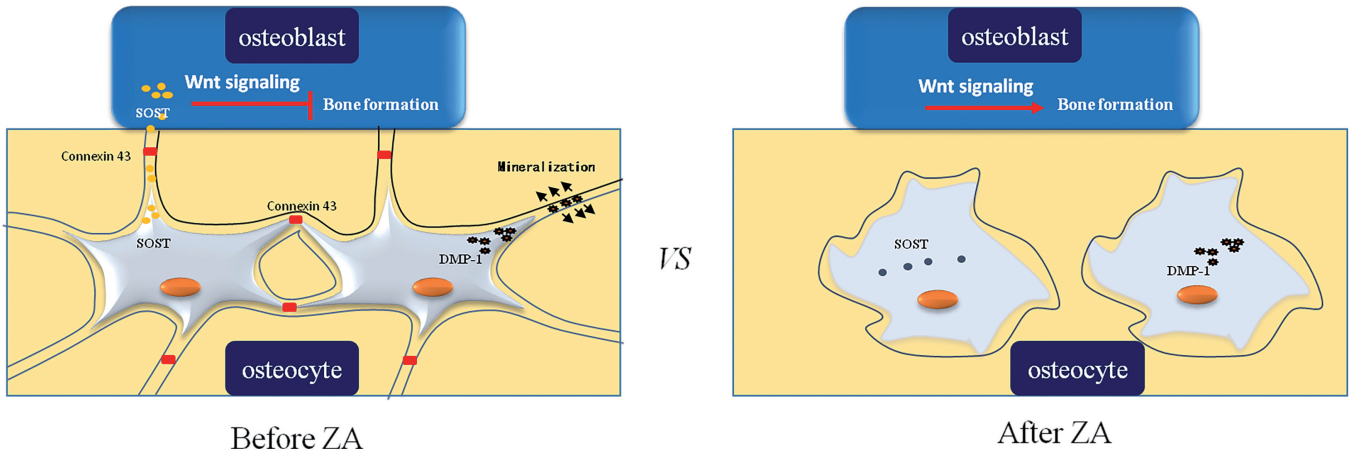

Fig. 6. A hypothetical scheme illustrating the influence of ZA during bone defect healing. ZA treatment reduces gap junction connections and blocked cellular communications between osteocytes and osteoblasts. The retaining of SOST in osteocyte leads to activation of Wnt signaling pathway and subsequent bone formation.

OLCS (Sasaki et al., 2013), we histochemically assessed osteocyte morphology and the OLCS distribution by DMP-1 staining. As shown in Fig. 4, ZA induced heterogeneous osteocytes and disturbed the distribution of the OLCS. Furthermore, according to the degree of OLCS regularity, DMP-1 reactivity had accumulated around osteocytes in the ZA group, but it was distributed evenly in the control group. These results may partly explain the impaired mineralization after ZA treatment. Considering that the OLCS serves as an important channel for information transmission from osteocytes to osteoblasts, we assume that the disappearance of negative regulation of bone formation from osteocytes through SOST can be at least partly interpreted as promotion of new bone in the ZA group. In addition, ZA-induced abnormal bone remodeling may further aggravate disorganization of the OLCS (Hirose et al., 2007; Ubaidus et al., 2009).

Osteocytes connect to each other and osteoblasts by their cytoplasmic processes interconnected through gap junctions (Doty, 1981; Shapiro, 1997). Connexin 43 (also known as GJA1) is a component of gap junctions and has important roles during cellular communication (John et al., 1999). N-BPs stimulate osteoblast proliferation and survival partly through regulation of connexin 43 hemichannel activity (Plotkin and Bellido, 2001). Alendronate has been reported to induce connexin 43 phosphorylation and therefore regulates its hemichannel activity, potentially through disassociation of connexin 43 with protein tyrosine phosphatase RPTPμ (Lezcano et al., 2014; Plotkin et al., 2002). In this study, we found that connexin 43 expression became sparse upon ZA treatment, which is consistent with the described blockade of communication between osteocytes and osteoblasts. In addition, connexin 43 has other functions such as regulating osteocyte cell survival, controlling the expression of osteocytic genes, and affecting bone remodeling (Bivi et al., 2012). Thus, the specific role of connexin 43 in this process and the signaling mechanisms of ZA affecting connexin 43 still need to be studied further.

Based on our data, we propose that ZA treatment reduces gap junction connections and blocks cellular communication between osteocytes and osteoblasts. Retaining SOST expression in osteocytes leads to activation of the Wnt signaling pathway and subsequent bone formation (Fig. 6). Our study provides a molecular insight to further understand the effects of N-BPs on the bone-remodeling process. It should be pointed out that there are many limitations in the current study. For example, differences between the animal model and humans are inevitable. It is hard to extrapolate data from animals to humans. We cannot accurately control the dosage of the medication used in animals to be similar to the dosage used in humans. Nonetheless, we expect to determine the mechanism of the effects of ZA on bone cells and the differences among various concentrations and diverse animal models, and to improve therapeutic protocols in future studies.

Acknowledgements. This study was partially supported by the National Nature Science Foundation of China (Grant Nos. 81271965; 81470719; 81611140133) to Li M and the Construction Engineering Special Fund of “Taishan Scholars” (No. Ts201511106) to Xu X.
Conflict of interest. The authors declare that they have no conflict of interest.

References

Aarden E.M., Burger E.H. and Nijweide P.J. (1994). Function of osteocytes in bone. J. Cell. Biochem. 55, 287-299.

Abu-Amer Y., Teitelbaum S.L., Chappel J.C., Schlesinger P. and Ross F.P. (1999). Expression and regulation of Rab3 proteins in osteoclasts and their precursors. J. Bone. Miner. Res.14, 1855-1860.

Balemans W., Ebeling M., Patel N., Van Hul E., Olson P., Dioszegi M., Lacza C., Wuyts W., Van Den Ende J., Willems P., Paes-Alves A.F., Hill S., Bueno M., Ramos F.J., Tacconi P., Dikkers F.G., Stratakis C., Lindpaintner K., Vickery B., Foernzler D. and Van Hul W. (2001). Increased bone density in sclerosteosis is due to the deficiency of a novel secreted protein (Sost). Hum. Mol. Genet. 10, 537-543.

Bellido T. and Plotkin L.I. (2011). Novel actions of bisphosphonates in bone: Preservation of osteoblast and osteocyte viability. Bone 49, 50-55.

Bivi N., Condon K.W., Allen M.R., Farlow N., Passeri G., Brun L.R., Rhee Y., Bellido T. and Plotkin L.I. (2012). Cell autonomous requirement of connexin 43 for osteocyte survival: Consequences for endocortical resorption and periosteal bone formation. J. Bone Miner. Res. 27, 374-389.

Burger E.H. and Klein-Nulend J. (1999). Mechanotransduction in bone--Role of the lacuno-canalicular network. FASEB. J.13, S101-S112.

Chen F. and Fu F. (2016). Safety of denosumab versus zoledronic acid in patients with bone metastases: A meta-analysis of randomized controlled trials. Oncol. Res. Treat. 39, 453-459.

Corrado A., Neve A., Maruotti N., Gaudio A., Marucci A. and Cantatore F.P. (2010). Dose-dependent metabolic effect of zoledronate on primary human osteoblastic cell cultures. Clin. Exp. Rheumatol. 28, 873-879.

Crane J.L., Xian L. and Cao X. (2016). Role of TGF-beta signaling in coupling bone remodeling. Methods. Mol. Biol. 1344, 287-300.

Doty S.B. (1981). Morphological evidence of gap junctions between bone cells. Calcif. Tissue. Int. 33, 509-512.

Feng J.Q., Ward L.M., Liu S., Lu Y., Xie Y., Yuan B., Yu X., Rauch F., Davi S.I., Zhang S., Rios H., Drezner M.K., Quarles L.D., Bonewald L.F. and White K.E. (2006). Loss of dmp1 causes rickets and osteomalacia and identifies a role for osteocytes in mineral metabolism. Nat. Genet. 38, 1310-1315.

Follet H., Li J., Phipps R.J., Hui S., Condon K. and Burr D.B. (2007). Risedronate and alendronate suppress osteocyte apoptosis following cyclic fatigue loading. Bone 40, 1172-1177.

Gao Y., Luo E., Hu J., Xue J., Zhu S. and Li J. (2009). Effect of combined local treatment with zoledronic acid and basic fibroblast growth factor on implant fixation in ovariectomized rats. Bone 44, 225-232.

Gerstenfeld L.C., Cullinane D.M., Barnes G.L., Graves D.T. and Einhorn T.A. (2003). Fracture healing as a post-natal developmental process: Molecular, spatial, and temporal aspects of its regulation. J.

Cell. Biochem. 88, 873-884.

Giuliani N., Pedrazzoni M., Passeri G., Negri G., Impicciatore M. and Girasole G. (1998). Bisphosphonates stimulate the production of basic fibroblast growth factor and the formation of bone marrow precursors of osteoblasts. New findings about their mechanism of action]. Minerva. Med. 89, 249-258.

Günes N., Dundar S., Saybak A., Artas G., Acikan I., Ozercan I.H., Atilgan S. and Yaman F. (2016). Systemic and local zoledronic acid treatment with hydroxyapatite bone graft: A histological and histomorphometric experimental study. Exp. Ther. Med. 12, 2417-2422.

Hirose S., Li M., Kojima T., de Freitas P.H., Ubaidus S., Oda K., Saito C. and Amizuka N. (2007). A histological assessment on the distribution of the osteocytic lacunar canalicular system using silver staining. J. Bone. Miner. Metab. 25, 374-382.

Itoh F., Aoyagi S., Furihata-Komatsu H., Aoki M., Kusama H., Kojima M. and Kogo H. (2003). Clodronate stimulates osteoblast differentiation in ST2 and MC3T3-E1 cells and rat organ cultures. Eur. J. Pharmacol. 477, 9-16.

Iwata K., Li J., Follet H., Phipps R.J. and Burr D.B. (2006). Bisphosphonates suppress periosteal osteoblast activity independently of resorption in rat femur and tibia. Bone 39, 1053-1058.

John G.R., Scemes E., Suadicani S.O., Liu J.S., Charles P.C., Lee S.C., Spray D.C. and Brosnan C.F. (1999). IL-1beta differentially regulates calcium wave propagation between primary human fetal astrocytes via pathways involving P2 receptors and gap junction channels. Proc. Natl. Acad. Sci. USA 96, 11613-11618.

Lezcano V., Bellido T., Plotkin L.I., Boland R. and Morelli S. (2014). Osteoblastic protein tyrosine phosphatases inhibition and connexin 43 phosphorylation by alendronate. Exp. Cell Res. 324, 30-39.

Li M., Hasegawa T., Hogo H., Tatsumi S., Liu Z., Guo Y., Sasaki M., Tabata C., Yamamoto T., Ikeda K. and Amizuka N. (2013). Histological examination on osteoblastic activities in the alveolar bone of transgenic mice with induced ablation of osteocytes. Histol. Histopathol. 28, 327-335.

Li X., Ominsky M.S., Niu Q.T., Sun N., Daugherty B., D'Agostin D., Kurahara C., Gao Y., Cao J., Gong J., Asuncion F., Barrero M., Warmington K., Dwyer D., Stolina M., Morony S., Sarosi I., Kostenuik P.J., Lacey D.L., Simonet W.S., Ke H.Z. and Paszty C. (2008). Targeted deletion of the SOST gene in mice results in increased bone formation and bone strength. J. Bone Miner. Res. 23, 860-869.

Lindtner R.A., Tiaden A.N., Genelin K., Ebner H.L., Manzl C., Klawitter M., Sitte I., von Rechenberg B., Blauth M. and Richards P.J. (2014). Osteoanabolic effect of alendronate and zoledronate on bone marrow stromal cells (BMSCs) isolated from aged female osteoporotic patients and its implications for their mode of action in the treatment of age-related bone loss. Osteoporos. Int. 25, 1151-1161.

Liu H., Cui J., Sun J., Du J., Feng W., Sun B., Li J., Han X., Liu B., Yimin, Oda K., Amizuka N. and Li M. (2015). Histochemical evidence of zoledronate Inhibiting c-Src expression and interfering with CD44/OPN-mediated osteoclast adhesion in the tibiae of mice. J. Mol. Histol. 46, 313-323.

Luckman S.P., Hughes D.E., Coxon F.P., Graham R., Russell G. and Rogers M.J. (1998). Nitrogen-containing bisphosphonates inhibit the mevalonate pathway and prevent post-translational prenylation of GTP-binding proteins, including Ras. J. Bone. Miner. Res. 13, 581-589.

Mardas N., Busetti J., de Figueiredo J.A., Mezzomo L.A., Scarparo R.K. and Donos N. (2017). Guided bone regeneration in osteoporotic conditions following treatment with zoledronic acid. Clin. Oral Implants Res. 26, 362-371.

Masuki H., Li M., Hasegawa T., Suzuki R., Ying G., Zhusheng L., Oda K., Yamamoto T., Kawanami M. and Amizuka N. (2010). Immunolocalization of DMP1 and SOST in the epiphyseal trabecule and diaphyseal cortical bone of osteoprotegerin deficient mice. Biomed. Res. 31, 307-318.

Oda K., Amaya Y., Fukushi-Irié M., Kinameri Y., Ohsuye K., Kubota I., Fujimura S. and Kobayashi J. (1999). A general method for rapid purification of soluble versions of glycosylphosphatidylinositol-anchored proteins expressed in insect cells: an application for human tissue-nonspecific alkaline phosphatase. J. Biochem. 126, 694-699.

Palokangas H., Mulari M. and Vaananen H.K. (1997). Endocytic pathway from the basal plasma membrane to the ruffled border membrane in bone-resorbing osteoclasts. J. Cell. Sci. 110, 1767-1780.

Phillips A.M. (2005). Overview of the fracture healing cascade. Injury 36, S5-S7.

Plotkin L.I. and Bellido T. (2001). Bisphosphonate-induced, hemichannel-hediated, anti-apoptosis through the Src/ERK pathway: A gap junction-independent action of connexin43. Cell. Commun. Adhes. 8, 377-382.

Plotkin L.I., Manolagas S.C. and Bellido T. (2002). Transduction of cell survival signals by connexin-43 hemichannels. J. Biol. Chem. 277, 8648-8657.

Rabelo G.D., Travencolo B.A., Oliveira M.A., Beletti M.E., Gallottini M. and Silveira F.R. (2015). Changes in cortical bone channels network and osteocyte organization after the use of zoledronic acid. Arch. Endocrinol. Metab. 59, 507-514.

Reinholz G.G., Getz B., Pederson L., Sanders E.S., Subramaniam M., Ingle J.N. and Spelsberg T.C. (2000). Bisphosphonates directly regulate cell proliferation, differentiation, and gene expression in human osteoblasts. Cancer Res. 60, 6001-6007.

Rochefort G.Y., Pallu S. and Benhamou C.L. (2010). Osteocyte: The unrecognized side of bone tissue. Osteoporos. Int. 21, 1457-1469.

Rodan G.A. (1998). Mechanisms of action of bisphosphonates. Annu. Rev. Pharmacol. Toxicol. 38, 375-388.

Rogers M.J. (2003). New insights into the molecular mechanisms of action of bisphosphonates. Curr. Pharm. Des. 9, 2643-2658.

Rogers M.J., Gordon S., Benford H.L., Coxon F.P., Luckman S.P., Monkkonen J. and Frith J.C. (2000). Cellular and molecular mechanisms of action of bisphosphonates. Cancer 88, 2961-2978.

Sasaki M., Hasegawa T., Yamada T., Hongo H., de Freitas P.H., Suzuki R., Yamamoto T., Tabata C., Toyosawa S., Yamamoto T., Oda K., Li M., Inoue N. and Amizuka N. (2013). Altered distribution of bone matrix proteins and defective bone mineralization in klotho-deficient mice. Bone 57, 206-219.

Shapiro F. (1997). Variable conformation of gap junctions linking bone cells: A transmission electron microscopic study of linear, stacked linear, curvilinear, oval, and annular junctions. Calcif. Tissue Int. 61, 285-293.

Stains J.P. and Civitelli R. (2005). Gap junctions in skeletal development and function. Biochim. Biophys. Acta 1719, 69-81.

Stains J.P., Watkins M.P., Grimston S.K., Hebert C. and Civitelli R. (2014). Molecular mechanisms of osteoblast/osteocyte regulation by

connexin43. Calcif. Tissue Int. 94, 55-67.

Tanaka T, Saito M, Chazono M, Kumagae Y, Kikuchi T, Kitasato S and Marumo K. (2010). Effects of alendronate on bone formation and osteoclastic resorption after implantation of beta-tricalcium phosphate. J. Biomed Mater Res. A. 93, 469-474.

Tanzer M., Karabasz D., Krygier J.J., Cohen R. and Bobyn J.D. (2005). The otto aufranc award: bone augmentation around and within porous implants by local bisphosphonate elution. Clin. Orthop. Relat. Res. 441, 30-39.

Tatsumi S., Ishii K., Amizuka N., Li M., Kobayashi T., Kohno K., Ito M., Takeshita S. and Ikeda K. (2007). Targeted ablation of osteocytes induces osteoporosis with defective mechanotransduction. Cell. Metab. 5, 464-475.

Toker H., Ozdemir H., Ozer H. and Eren K. (2012). A comparative evaluation of the systemic and local alendronate treatment in synthetic bone graft: A histologic and histomorphometric study in a rat calvarial defect model. Oral Surg. Oral Med. Oral.114, S 146-152.

Toyosawa S., Shintani S., Fujiwara T., Ooshima T., Sato A., Ijuhin N. and Komori T. (2001). Dentin matrix protein 1 is predominantly expressed in chicken and rat osteocytes but not in osteoblasts. J. Bone Miner. Res. 16, 2017-2026.

Tsuboi K., Hasegawa T., Yamamoto T., Sasaki M., Hongo H., de Freitas P.H., Shimizu T., Takahata M., Oda K., Michigami T., Li M., Kitagawa Y. and Amizuka N. (2016). Effects of drug discontinuation after short-term daily alendronate administration on osteoblasts and osteocytes in mice. Histochem. Cell. Biol. 146, 337-350.

Ubaidus S., Li M., Sultana S., de Freitas P.H., Oda K., Maeda T., Takagi R. and Amizuka N. (2009). FGF23 is mainly synthesized by osteocytes in the regularly distributed osteocytic lacunar canalicular system established after physiological bone remodeling. J. Electron. Microsc (Tokyo) 58, 381-392.

Weinbaum S., Cowin S.C. and Zeng Y. (1994). A model for the excitation of osteocytes by mechanical loading-induced bone fluid shear stresses. J. Biomech. 27, 339-360.

Winkler D.G., Sutherland M.K., Geoghegan J.C., Yu C., Hayes T., Skonier J.E., Shpektor D., Jonas M., Kovacevich B.R., Staehling-Hampton K., Appleby M., Brunkow M.E. and Latham J.A. (2003). Osteocyte control of bone formation via SOST, a novel bmp antagonist. EMBO. J. 22, 6267-6276.

Yao W., Cheng Z., Pham A., Busse C., Zimmermann E.A., Ritchie R.O., and Lane N.E. (2008). Glucocorticoid-induced bone loss in mice can be reversed by the actions of parathyroid hormone and risedronate on different pathways for bone formation and mineralization. Arthritis. Rheum. 58, 3485-3497.

Yu Y.Y., Lieu S., Hu D., Miclau T. and Colnot C. (2012). Site specific effects of zoledronic acid during tibial and mandibular fracture repair. PLoS. One 7, e31771.

Accepted March 27, 2017